

SYNCHRONIZATION ERROR MINIMIZATION USING SPECTRAL CHARACTERISTICS AND DWT DENOISING FOR COOPERATIVE COMMUNICATION NETWORKS

ANAND RANJAN^{1*}, O.P. SINGH², HIMANSHU KATIYAR³

¹Department of Electronics and Communication Engineering, Amity School of Engineering and Technology (ASET), AMITY University, Lucknow Campus, Uttar Pradesh, India.

²Department of Electrical and Electronics Engineering, Amity School of Engineering and Technology (ASET), AMITY University, Lucknow Campus, Uttar Pradesh, India.

³Department of Electronics Engineering, Rajkiya Engineering College, Sonbhadra, Uttar Pradesh, India.

*anandranjan@live.com, opsingh@amity.edu, katiyarhimanshu@gmail.com

ABSTRACT

The application of a cooperative communication system with a source, relay, and destination is discussed, along with a sensor data-aided DWT-based symbol timing synchronization. For low value of the signal-to-noise ratio (SNR) cases, a power spectrum estimation error correction is carried out. Cross spectral density based modal shape application uses timing synchronization using DFT property, and the results are compared. It is demonstrated that the cross power spectrum modal shape error is significantly reduced or insignificant when time synchronization is performed using DWT denoising. The benefit of diversity in cooperative communication may be lost over long periods of time due to a little time lag, it has been noted. It has been found that a large correction can be achieved by combining the DFT time lag correction properties with the DWT denoising method. The sensor response in the cooperative communication system faces high level of anomaly in spectral estimates due to error in sampling time of sensor nodes. Since the sensor nodes are of low hardware complexity hence simple but accurate methods are very challenging to find in wireless communication applications. This paper aims to: i) minimize the mismatch in sampling delay between sensor nodes to mitigate their impact on the global synchronization error of the cooperative communication network; ii) simulate and validate spectral characteristics based sampled sequences delay correction that enable the high accuracy in estimate of sample time mismatch on every node and calculation of modal value of sensor data frequency response; and iii) evaluate the conditions for nodes employing DWT based denoising prior to correction of time delay shift.

KEYWORDS: *Symbol Timing Error* , *Cooperative Communications* , *DWT Denoising* , *Timing Synchronization* .

1 INTRODUCTION

Due to its capacity to realize the performance gains of multiple-input multiple-output (MIMO) systems the single antenna in the cooperative communications concept attracted a lot of attention [1-3]. A wireless network's capacity, symbol error rate performance, and energy efficiency can all be improved via cooperative diversity communications [4-6]. Many studies on cooperative communications, however, used the assumption that the receiver would have perfect symbol synchronization, which is exceedingly challenging given the scattered nature of the field. In real-world operating situations, such an

assumption is very rarely true. The theoretical and numerical results on performance decline due to problems due to synchronization in a cooperative network [7-10]. The timing synchronization impact examined in a cooperative multiple input single output applications [8], and observations shows that the timing errors are significant since the benefit of cooperation is eliminated in terms of diversity gain. In [9], it is demonstrated that as the performance of relays placed in parallel degrades gradually when problems of synchronization are modest, the deterioration of the performance is high when synchronization loss are big. The issue related to timing matching and estimation of channel as well as the resynchronization of

numerous offsets in timing in a cooperative relay system are focused [11], but the impact on the performance of combining methods was left out. Researchers have offered delay-robust transmission systems as a way to get around the synchronization issue [12–14]. Despite their potential, these techniques have limitations on transmitting and cooperating, which restricts their applicability. However, a lot of the transmission strategies used today and associated demodulation techniques presuppose that the cooperative users are synchronised in time. Timing synchronization problems receive far less attention than synchronization of the frequency and estimation of channel behavior in cooperative communication systems, as discussed by [15–20]. In this work, analysis is performed of a multiple node cooperative communication scheme using sensor nodes and relaying nodes, using cascading two techniques, and timing synchronization error is minimized for each transmission between the nodes. The work done here for a cooperative system is extended by a data-aided DWT noise with DFT time time lag characteristics correction scheme that is demonstrated by contrasting it with a

cross-power spectrum modal shape estimate. An advantage of the suggested scheme is depicted as simplicity in computational execution. The timing synchronization performance control and timing synchronization scheme performance are examined with and without DWT denoising in terms of frequency and peak error in cross-power spectrum density modal shape. The impact of minimizing synchronization faults on cooperative communications and presented. Timing synchronization is found to have a considerable impact on the output. The work is associated with cooperative communication networks which are energy efficient but incorporates multiple device at different functioning at a same time. They use relay nodes to enhance signal power. Since these schemes are latest and few work is available in dealing with the error occurs due to synchronization losses. The available literatures generally focus on simple WSN system having similar type of devices at homogeneous hardware property.

2 WSN BASED ON COOPERATIVE COMMUNICATION SYSTEM :

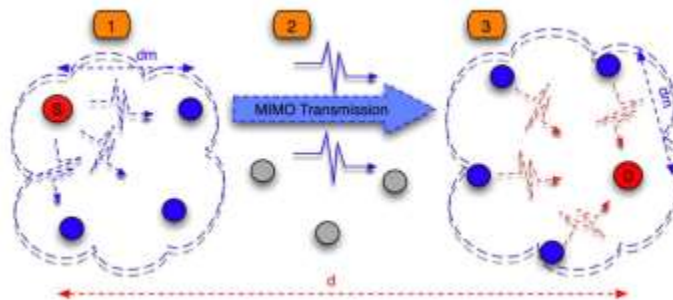


Figure 1: Cooperative Communication Application In WSN

As shown in Fig. 1, there are three phases to the MIMO based data transmission in cooperative network over distance d in between destination node D and source node S for fulfilling the purpose of exchange of data locally, cooperative mode transmission with MIMO approach and reception at cooperative communication scheme. Node S cooperates to the surrounding neighbours for data transmission side in order to exchanging the information (the cooperating nodes in between distance is assumed to be d_m is lower than the transmission distance d). Following that, STBC methods are used, much like conventional MIMO systems, to concurrently encode and send the data blocks to the single or multiple destination cooperative nodes (each cooperative

node acts as an antenna for the MIMO based transmission structure). At the receiver end, the neighbours in cooperative network for the destination side i.e. D take in the modulated symbols under MIMO coding schemes & then recursively transmit these generated symbols to D node for combining of the MIMO signals. A cooperative MIMO system's performance is hampered by the synchronisation error during sending on the cooperative transmitter side and the presence of additive noise on the cooperative receiver side since the nodes are physically apart. With the number of transmitter-receiver antennas are same, the system's of cooperative network has larger BER than the classic system's with MIMO schemes due to performance degradation.

3.1 Power Spectral Density:

Power spectral density is a measurement of a signal's power intensity in the frequency domain (PSD). In practice, the PSD is computed from the FFT spectrum of a signal. The PSD is a useful tool for summarizing the amplitude-versus-frequency information of a random event. For the Random signals the PSDs are utilized to represent the control and input channel signals. Random vibration is a common occurrence in the physical universe. Traveling in the car, transportation in the a truck, or in an aero plane or ship will cause random vibrations to be felt. The motion is synchronous at several frequencies. Over time, the amplitudes of these frequencies vary unpredictably. Most often, random motion is described in terms of its Power Spectral Density. By the use of graphic PSD represents random vibration in both the temporal and frequency domains.

Determining the typical value of the relative change of amplitudes inside a specific frequency range is the solution. Even while the speed increase sufficiency at a certain spectral information actually changes over time, its average value will generally stay quite constant. With the help of a vibration test framework, one can successfully duplicate random signals for the depiction of the irregular cycle. The research of irregular variations of the power utilized in an electrical circuit gave rise to the a similar idea that is relevant to mechanical vibration applications. Vibration testing typically makes use of speed increase estimations, however, the several application has adopted "PSD". The sufficiency advantages of a PSD are frequently presented in g^2/Hz for vibration testing. What significance do these units actually have? By examination, lb/in^2 , a unit of stress. It is a typical unit in designing application. A unit of g^2/Hz has a poor initial appearance because it isn't obvious as a real number. The range is calculated in g^2 units, and Hz (frequency) is a normalization factor. The time information is obtained and then converted entirely to a spectral range in the control framework using an FFT calculation.

3.2 Discrete Wavelet Transform (Dwt) :

DWT is a time-spectrum transformation method with several goals that can show the incompleteness of time and spectral domain. The main concept is the decomposition of the signal into smaller signals with different space and

spectrum, after which the coefficient is dealt with.

A multistage change can be used to implement the DWT. At level 1 in the DWT space, a signal is divided into two subgroups denoted by the letters L and H where L stands for coarse-level coefficients and the other address the best scale wavelet coefficients.

Wavelets are special capabilities that are used as the fundamental capabilities for addressing signals, with a structure undifferentiated from sines and cosines in Fourier analysis [7]. The sub-band L addresses the coarse-scale DWT coefficients while the sub-groups H address the fine-size of DWT coefficients. To acquire the following coarser size of wavelet coefficients, the sub-band L is additionally handled until some last scale N is reached. At the point when N is arrived at we will have $3N+1$ sub-groups comprising of the multi-goal sub-groups L_N and H_x where x reaches from 1 until N. Because of its superb spatio-recurrence limitation properties, the DWT is entirely reasonable to distinguish the signals. Specifically, this property permits the double-dealing of the concealing impact in time and frequency Overall the majority of the signal energy is gathered at the lower frequency sub-groups L_x and in this manner deterioration of data in these sub-groups might corrupt the signal altogether. The low frequency sub-groups contribute to high power content fundamentally. Then again, the high frequency sub-groups H_x incorporate the minute details of the signal and the by human perception is not capable to observe delicate changes in such sub-groups. This permits the noise suppression to be implanted in this sub group. The trade off embraced by numerous DWT-based calculation, is to implant the noise removal in the center frequency sub-groups [15].

3.3 Welch Method:

in Digital Signal processing PSD has very significant applications . Welch method is the modification of the Bartlett method. In this method the data segment are represented by

$$s_i(k) = \{s(k + iD) , k: 1 \text{ to } M - 1\} \quad (1)$$

Here $i.D$ represents starting point of i^{th} sample. If $D = 0$ then M , the no segment overlapping occurs and the L of data sequence is the segment length.

The second modification in is applying the window on the data segments before applying the periodogram.

$$P_{ss,i}(f) = \left| \sum_{k=0}^{M-1} x(k)\omega(k)exp^{-i.\omega.n} \right|^2 / M \quad (2)$$

The Welch power spectrum estimate is the average of modified periodgram. The goal of assessed power assessment is decide by the unearthy goal of each section which is of length L. It is window subordinate.

3.4 Causes behind error in synchronization:

The following factors could contribute to synchronous loss at the nodes in the IOT: (a) synchronization errors of internal clock; (b) non-simultaneous startup time; (c) variations in sample frequency among the nodes and (d) non-uniformity in the sampling time in time domain. The time series should sampled ideally in synchronized manner and evenly (with a constant sampling time gap known as T_s) (all the nodes starts to sense at the globally similar time). At k^{th} .sampling instant, the time is:

$$t_k = kT_s \quad (3)$$

But the k^{th} signal in real time sampled at a separate instant of time for the reasons listed above.

$$t'_k = k.T_s + \delta + c.k + \varepsilon(k) \quad (4)$$

where the clock synchronization error is rather modest and comes from sources (a) and (b), and where is a constant time shift; only sensor start delay time is taken into consideration here. Non-uniform sampling is caused by these time jitters, which include ck , a linear shifting in time at transmitter (c), the coefficient c representation of random shift in time at source (d), and (k), a random time shift from source (c) [21- 23].

3.5 Proposed Algorithm

Direct intuition recommends recreating the synchronous samples in cooperative communication network from measured non-synchronous ones in order to remove the synchronization flaws at relay node. This is referred to as signal reconstruction, and research has been done in this direction. Instead of rebuilding time frame, we provide a correction technique at relay node to restore the true PSD value in the spectral frame for cooperative communication network. The majority of modal identification algorithms simply require spectral densities or correlation functions. By using IFFT,

we can also readily extract the correlation functions as long as we have access to adjusted PSD.

3.5.1 Case of constant shift in time domain:

We have considered two signals

$$\{ x_\alpha(0), x_\alpha(\Delta t), \dots, x_\alpha((N-1)\Delta t) \}^T \text{ and } \{ x_\beta(0), x_\beta(\Delta t), \dots, x_\beta((N-1)\Delta t) \}^T$$

and i.e., x'_β has a constant shift in time named as δ . The discrete Fourier transform (DFT) of x_α is given by:

$$X_\alpha(\omega_k) = \sum_{n=0}^{n=N-1} x_\alpha(n\Delta t)exp^{-\omega_k.j.\Delta t.n} \quad (5)$$

$$\omega_k = \Delta\omega.k, \Delta\omega = 2.\pi/N.\Delta t, k=0 \text{ to } N/2.$$

The DFT for the shifted signal x'_β is given by:

$$X'_\beta(\omega_k) = exp^{-\omega_k.j.\delta}. X_\beta(\omega_k), \quad (6)$$

where $X_\beta(\omega_k)$ is the DFT of the original signal. Then, the true cross spectral density estimation value obtained as:

$$S_{x_\alpha, \beta}(\omega_k) = \Delta t. E(X_\alpha(\omega_k). X^*_\beta(\omega_k)) / N, \text{ where } * \text{ denotes complex conjugate operator.}$$

3.5.2 Linear time shift:

In a cooperative communication network let us consider two time histories $x_\alpha(n)$ and $x_\beta(n)$ with the difference in sampling frequencies such that Δt_α is not equal to Δt_β and with corresponding sampling time of $T_\alpha = \Delta t_\alpha.N_\alpha$ and $T_\beta = \Delta t_\beta.N_\beta$. In DFT it is known that $\omega_k = k.\Delta\omega$. In order to ensure that X_α and X_β are corresponding to the same discrete frequency when calculating the cross spectral density, their resolutions of frequency must be same at sink in cooperative communication network, i.e., $\Delta\omega_\alpha$ approximately $\Delta\omega_\beta$, thus the time of duration must be almost same, hence:

$$N_\alpha.\Delta t_\alpha = N_\beta.\Delta t_\beta \quad (7)$$

On the basis of this relation, the cross PSD is estimated as:

$$S_{x_\alpha, \beta}(\omega_k) = \Delta t_\alpha. \frac{E(X_\alpha(\omega_k). X^*_\beta(\omega_k))}{N_\alpha} = \Delta t_\beta. \frac{E(X_\alpha(\omega_k). X^*_\beta(\omega_k))}{N_\beta} \quad (8)$$

3.6 Algorithm:

Non-synchronous data actually undergoes a combination of linear and constant time changes in cooperative communication network. To calculate the accurate power spectral density estimate from non-synchronous data in IOT, follow these steps:

- (1) Before conducting a sensing experiment, calibrate the sample frequencies of each sensor board in cooperative communication network.
- (2) Conduct a sensing experiment and remember to sample with time stamps.
- (3) Divide the data into several parts using one sensor as the reference. There are N_r data points in each segment.
- (4) Separate the information from other sensors into several groups as well. The first data point of each segment is chosen to be as similar as possible to the first data point of the corresponding segment in the reference sensor data by comparing their time stamps. The length N_i of each segment is chosen to substantially satisfy Eq. (7).
- (5) Determine each segment's Fourier transform and use Eq. to fix it (5) at the relay node of cooperative communication network.
- (6) Use Eq. to determine the cross spectral density (8) at the relay node.

4 RESULT AND DISCUSSION:

In this section, simulations of the MATLAB programming environment are used to analyse non-synchronous sensor behavior and modal identification in cooperative communication network. An example that uses simulated data to illustrate the novel denoising using the wavelet for accurate estimation of cross power spectral density for eradicating errors in synchronization is provided. All the signals are sampled with a T_s as a constant sampling time gap of in a cooperative communication network environment, and all the sensors are simulated to start sensing at the same time. Clock synchronization error, non-simultaneous sensing start-up time, differences in sampling frequency of the sensor nodes, and non-uniform sampling interval with respect to time are the potential sources behind non-synchronous sensing that are taken into consideration in this work for cooperative communication network applications.

The k^{th} data point is really sampled at a distinct time instant for the reasons indicated above:

$$t_k' = k.T_s + \delta + ck + \varepsilon(k) \quad (1)$$

The continuous time shift, emanating from transmitter; as a result, in this situation, just the delay in start-up of sensing is taken into consideration.

The difference between the real sampling time and the nominal sampling time is represented by the coefficient ck , which stands for linear time shift.

(k) in above equation is the random time shift; it is due to the jitters in time leading to a non-uniform sampling type error.

The values that are specified in the algorithm are as per the aforementioned parameter definitions:

Sampling duration in seconds is given by $T_s = 0.0250$ s. Number of sensors are considered here is $N = 15$

b) Error at the startup time of sensors; δ in seconds = [-0.000 7266 -0.00025469 -0.000 3046 -0.000 8956 0.000 80 87 -0.00027760 0.000 8462 0.000 0497 -0.000 9706 0.0007200 5 0.0008238 0.00058052 0.00020924 -0.000 0 276 0.000 0895].

c) the difference in the sample frequency: in the case of baseline there is negligible time shift; $c_{10} = 0$, for the constant time case shift $c_2 = 0.02$ seconds & for linear time shift in seconds the assumptions are : $f_{s0} = 40.48$ hertz $f_{s2} = 39.84$ hz $T_{s0} = 0.0246$ secs. $T_{s2} = 0.02500$ seconds

c_3 (seconds) = [0.0002980 0.000299990 - 0.000002000 -0.000002000 0.00029997 0.00029999 -0.000002000 -0.000002000 - 0.000002000 -0.000002000 0.000299980 - 0.000002000 0.000299981 -0.000002000 0.000299978].

Table 4.1: Sensing Time Of Sensors Id From 1 To 10 With The Linear Time Shift For Cooperative Communication.

Sample	Sensor Id S1 to S10									
	S1	S2	S3	S4	S5	S6	S7	S8	S9	S10
1	0.0003	0.0003	-0.0000	-0.0000	0.0003	0.0003	-0.0000	-0.0000	-0.0000	-0.0000
2	0.0006	0.0006	-0.0002	-0.0002	0.0006	0.0006	-0.0002	-0.0002	-0.0002	-0.0002
3	0.0009	0.0009	-0.0003	-0.0003	0.0009	0.0009	-0.0003	-0.0003	-0.0003	-0.0003
4	0.0002	0.0002	-0.0004	-0.0004	0.0002	0.0002	-0.0004	-0.0004	-0.0004	-0.0004
5	0.0005	0.0005	-0.0005	-0.0005	0.0005	0.0005	-0.0005	-0.0005	-0.0005	-0.0005
6	0.0008	0.0008	-0.0006	-0.0006	0.0008	0.0008	-0.0006	-0.0006	-0.0006	-0.0006
7	0.0020	0.0020	-0.0007	-0.0007	0.0020	0.0020	-0.0007	-0.0007	-0.0007	-0.0007
8	0.0024	0.0024	-0.0008	-0.0008	0.0024	0.0024	-0.0008	-0.0008	-0.0008	-0.0008
9	0.0027	0.0027	-0.0009	-0.0009	0.0027	0.0027	-0.0009	-0.0009	-0.0009	-0.0009
10	0.003	0.003	-0.000	-0.000	0.003	0.003	-0.000	-0.000	-0.000	-0.000
11	0.0033	0.0033	-0.0000	-0.0000	0.0033	0.0033	-0.0000	-0.0000	-0.0000	-0.0000
12	0.0036	0.0036	-0.0002	-0.0002	0.0036	0.0036	-0.0002	-0.0002	-0.0002	-0.0002
13	0.0039	0.0039	-0.0003	-0.0003	0.0039	0.0039	-0.0003	-0.0003	-0.0003	-0.0003
14	0.0042	0.0042	-0.0004	-0.0004	0.0042	0.0042	-0.0004	-0.0004	-0.0004	-0.0004
15	0.0045	0.0045	-0.0005	-0.0005	0.0045	0.0045	-0.0005	-0.0005	-0.0005	-0.0005
16	0.0048	0.0048	-0.0006	-0.0006	0.0048	0.0048	-0.0006	-0.0006	-0.0006	-0.0006
17	0.0050	0.0050	-0.0007	-0.0007	0.0050	0.0050	-0.0007	-0.0007	-0.0007	-0.0007
18	0.0054	0.0054	-0.0008	-0.0008	0.0054	0.0054	-0.0008	-0.0008	-0.0008	-0.0008
19	0.0057	0.0057	-0.0009	-0.0009	0.0057	0.0057	-0.0009	-0.0009	-0.0009	-0.0009
20	0.006	0.006	-0.002	-0.002	0.006	0.006	-0.002	-0.002	-0.002	-0.002
20	0.0063	0.0063	-0.0020	-0.0020	0.0063	0.0063	-0.0020	-0.0020	-0.0020	-0.0020
22	0.0066	0.0066	-0.0022	-0.0022	0.0066	0.0066	-0.0022	-0.0022	-0.0022	-0.0022
23	0.0069	0.0069	-0.0023	-0.0023	0.0069	0.0069	-0.0023	-0.0023	-0.0023	-0.0023
24	0.0072	0.0072	0.0024	0.0024	0.0072	0.0072	0.0024	0.0024	0.0024	0.0024
25	0.0075	0.0075	0.0025	0.0025	0.0075	0.0075	0.0025	0.0025	0.0025	0.0025
26	0.0078	0.0078	0.0026	0.0026	0.0078	0.0078	0.0026	0.0026	0.0026	0.0026
27	0.0080	0.0080	0.0027	0.0027	0.0080	0.0080	0.0027	0.0027	0.0027	0.0027



			0	0			0	0	0	0
28	0.008 4	0.00839 9	- 0.0028 0	- 0.0028 0	0.00839 9	0.00839 9	- 0.0028 0	- 0.0028 0	- 0.0028 0	- 0.0028 0
29	0.008 7	0.00869 9	- 0.0029 0	- 0.0029 0	0.00869 9	0.00869 9	- 0.0029 0	- 0.0029 0	- 0.0029 0	- 0.0029 0
30	0.009	0.00899 9	- 0.0030 0	- 0.0030 0	0.00899 9	0.00899 9	- 0.0030 0	- 0.0030 0	- 0.0030 0	- 0.0030 0
30	0.009 3	0.00929 9	-0.0030 0	-0.0030 0	0.00929 9	0.00929 9	-0.0030 0	-0.0030 0	-0.0030 0	-0.0030 0
32	0.009 6	0.00959 9	- 0.0032 0	- 0.0032 0	0.00959 9	0.00959 9	- 0.0032 0	- 0.0032 0	- 0.0032 0	- 0.0032 0
33	0.009 9	0.00989 9	- 0.0033 0	- 0.0033 0	0.00989 9	0.00989 9	- 0.0033 0	- 0.0033 0	- 0.0033 0	- 0.0033 0
34	0.00 02	0.00 00 99	- 0.0034 0	- 0.0034 0	0.00 00 99	0.00 00 99	- 0.0034 0	- 0.0034 0	- 0.0034 0	- 0.0034 0
35	0.00 05	0.00 0499	- 0.0035 0	- 0.0035 0	0.00 0499	0.00 0499	- 0.0035 0	- 0.0035 0	- 0.0035 0	- 0.0035 0
36	0.00 08	0.00 0799	- 0.0036 0	- 0.0036 0	0.00 0799	0.00 0799	- 0.0036 0	- 0.0036 0	- 0.0036 0	- 0.0036 0
37	0.00 0 0	0.00 0 099	- 0.0037 0	- 0.0037 0	0.00 0 099	0.00 0 099	- 0.0037 0	- 0.0037 0	- 0.0037 0	- 0.0037 0
38	0.00 0 4	0.00 0 399	- 0.0038 0	- 0.0038 0	0.00 0 399	0.00 0 399	- 0.0038 0	- 0.0038 0	- 0.0038 0	- 0.0038 0
39	0.00 0 7	0.00 0 699	- 0.0039 0	- 0.0039 0	0.00 0 699	0.00 0 699	- 0.0039 0	- 0.0039 0	- 0.0039 0	- 0.0039 0
40	0.00 2	0.00 0 999	- 0.0040 0	- 0.0040 0	0.00 0 999	0.00 0 999	- 0.0040 0	- 0.0040 0	- 0.0040 0	- 0.0040 0
40	0.00 23	0.00 2299	-0.0040 0	-0.0040 0	0.00 2299	0.00 2299	-0.0040 0	-0.0040 0	-0.0040 0	-0.0040 0
42	0.00 26	0.00 2599	- 0.0042 0	- 0.0042 0	0.00 2599	0.00 2599	- 0.0042 0	- 0.0042 0	- 0.0042 0	- 0.0042 0
43	0.00 29	0.00 2899	- 0.0043 0	- 0.0043 0	0.00 2899	0.00 2899	- 0.0043 0	- 0.0043 0	- 0.0043 0	- 0.0043 0
44	0.00 32	0.00 30 99	- 0.0044 0	- 0.0044 0	0.00 30 99	0.00 30 99	- 0.0044 0	- 0.0044 0	- 0.0044 0	- 0.0044 0
45	0.00 35	0.00 3499	- 0.0045 0	- 0.0045 0	0.00 3499	0.00 3499	- 0.0045 0	- 0.0045 0	- 0.0045 0	- 0.0045 0
46	0.00 38	0.00 3799	- 0.0046 0	- 0.0046 0	0.00 3799	0.00 3799	- 0.0046 0	- 0.0046 0	- 0.0046 0	- 0.0046 0
47	0.00 40	0.00 4099	- 0.0047 0	- 0.0047 0	0.00 4099	0.00 4099	- 0.0047 0	- 0.0047 0	- 0.0047 0	- 0.0047 0
48	0.00	0.00	-	-	0.00	0.00	-	-	-	-



	44	4399	0.0048 0	0.0048 0	4399	4399	0.0048 0	0.0048 0	0.0048 0	0.0048 0
49	0.00 47	0.00 4699	- 0.0049 0	- 0.0049 0	0.00 4699	0.00 4699	- 0.0049 0	- 0.0049 0	- 0.0049 0	- 0.0049 0
50	0.00 5	0.00 4999	- 0.0050 0	- 0.0050 0	0.00 4999	0.00 4999	- 0.0050 0	- 0.0050 0	- 0.0050 0	- 0.0050 0

As the loss in synchronization occurs and most of the nodes starts responding at various times as a result of the sensing delay in the cooperative communication network. The error between ideal

and real sensing time grows as the sample instants are increased on receiving at relay node in cooperative communication network, as shown in table 4.2.

Table 4.2: Ideal And Actual Sampling Time Instants Of 1 To 9 Sensors.

Sampling instants	Ideal sampling Time	Actual Sampling Time Of sensor nodes								
		S1	S2	S3	S4	S5	S6	S7	S8	S9
1	0.0 2 5	0.0 2 5	0.0 2 4	0.0 24	0.0 23	0.0 23	0.024	0.026	0.026	0.026
2	0.0 5	0.0 5	0.04 8	0.04 9	0.0 48	0.0 48	0.0 48	0.0 50	0.0 52	0.0 52
3	0.0 75	0.0 76	0.0 73	0.0 74	0.0 73	0.0 73	0.0 73	0.0 76	0.0 77	0.0 77
4	0. 0	0. 0 00	0.098	0.099	0.098	0.098	0.098	0.0 02	0.0 02	0.0 02
5	0.0 25	0.0 26	0.0 23	0.0 24	0.0 23	0.0 23	0.0 23	0.0 27	0.0 27	0.0 28
6	0.0 5	0.0 52	0.0 48	0.0 49	0.0 48	0.0 48	0.0 48	0.0 52	0.0 53	0.0 53
7	0.0 75	0.0 77	0.0 73	0.0 74	0.0 72	0.0 73	0.0 73	0.0 78	0.0 78	0.0 78
8	0.2	0.202	0.0 98	0.0 99	0.0 97	0.0 98	0.0 98	0.203	0.203	0.204
9	0.225	0.228	0.223	0.223	0.222	0.222	0.223	0.228	0.229	0.229
10	0.25	0.253	0.248	0.248	0.247	0.247	0.248	0.254	0.254	0.254
11	0.275	0.278	0.273	0.273	0.272	0.272	0.273	0.279	0.279	0.279
12	0.3	0.303	0.297	0.298	0.297	0.297	0.297	0.304	0.305	0.305
1 3	0.325	0.329	0.322	0.323	0.322	0.322	0.322	0.329	0.33	0.33
1 4	0.35	0.354	0.347	0.348	0.347	0.347	0.347	0.355	0.355	0.355
1 5	0.375	0.379	0.372	0.373	0.372	0.372	0.372	0.38	0.38	0.380
1 6	0.4	0.405	0.397	0.398	0.397	0.397	0.397	0.405	0.406	0.406
1 7	0.425	0.43	0.422	0.423	0.420	0.422	0.422	0.430	0.430	0.430
1 8	0.45	0.455	0.447	0.448	0.446	0.447	0.447	0.456	0.456	0.457
1 9	0.475	0.480	0.472	0.472	0.470	0.470	0.472	0.480	0.482	0.482
20	0.5	0.506	0.497	0.497	0.496	0.496	0.497	0.507	0.507	0.507
20	0.525	0.530	0.522	0.522	0.520	0.520	0.522	0.532	0.532	0.532
22	0.55	0.556	0.546	0.547	0.546	0.546	0.546	0.557	0.558	0.558
23	0.575	0.582	0.570	0.572	0.570	0.570	0.570	0.582	0.583	0.583
24	0.6	0.607	0.596	0.597	0.596	0.596	0.596	0.608	0.608	0.608
25	0.625	0.632	0.620	0.622	0.620	0.620	0.620	0.633	0.633	0.634
26	0.65	0.658	0.646	0.647	0.646	0.646	0.646	0.658	0.659	0.659
27	0.675	0.683	0.670	0.672	0.67	0.670	0.670	0.684	0.684	0.684
28	0.7	0.708	0.696	0.697	0.695	0.696	0.696	0.709	0.709	0.70
29	0.725	0.734	0.720	0.720	0.72	0.72	0.720	0.734	0.735	0.735
30	0.75	0.759	0.746	0.746	0.745	0.745	0.746	0.76	0.76	0.76
30	0.775	0.784	0.770	0.770	0.77	0.77	0.770	0.785	0.785	0.785
32	0.8	0.809	0.795	0.796	0.795	0.795	0.795	0.80	0.80 0	0.80 0

33	0.825	0.835	0.82	0.820	0.82	0.82	0.82	0.835	0.836	0.836
34	0.85	0.86	0.845	0.846	0.845	0.845	0.845	0.860	0.860	0.860
35	0.875	0.885	0.87	0.870	0.87	0.87	0.87	0.886	0.886	0.887
36	0.9	0.90 0	0.895	0.896	0.895	0.895	0.895	0.90 0	0.90 2	0.90 2
37	0.925	0.936	0.92	0.920	0.90 9	0.92	0.92	0.937	0.937	0.937
38	0.95	0.960	0.945	0.946	0.944	0.945	0.945	0.962	0.962	0.963
39	0.975	0.987	0.97	0.97	0.969	0.969	0.97	0.987	0.988	0.988
40	0	0.00 2	0.995	0.995	0.994	0.994	0.995	0.00 3	0.00 3	0.00 3
40	0.025	0.037	0.02	0.02	0.00 9	0.00 9	0.02	0.038	0.038	0.038
42	0.05	0.062	0.044	0.045	0.044	0.044	0.044	0.063	0.064	0.064
43	0.075	0.088	0.069	0.07	0.069	0.069	0.069	0.088	0.089	0.089
44	0.0	0.00 0	0.094	0.095	0.094	0.094	0.094	0.00 4	0.00 4	0.00 4
45	0.0 25	0.0 38	0.00 9	0.0 2	0.00 9	0.00 9	0.00 9	0.0 39	0.0 39	0.0 4
46	0.0 5	0.0 64	0.0 44	0.0 45	0.0 44	0.0 44	0.0 44	0.0 64	0.0 65	0.0 65
47	0.0 75	0.0 89	0.0 69	0.0 7	0.0 68	0.0 69	0.0 69	0.0 9	0.0 9	0.0 9
48	0.2	0.20 4	0.0 94	0.0 95	0.0 93	0.0 94	0.0 94	0.20 5	0.20 5	0.20 6
49	0.225	0.24	0.20 9	0.20 9	0.20 8	0.20 8	0.20 9	0.24	0.240	0.240
50	0.25	0.265	0.244	0.244	0.243	0.243	0.244	0.266	0.266	0.266

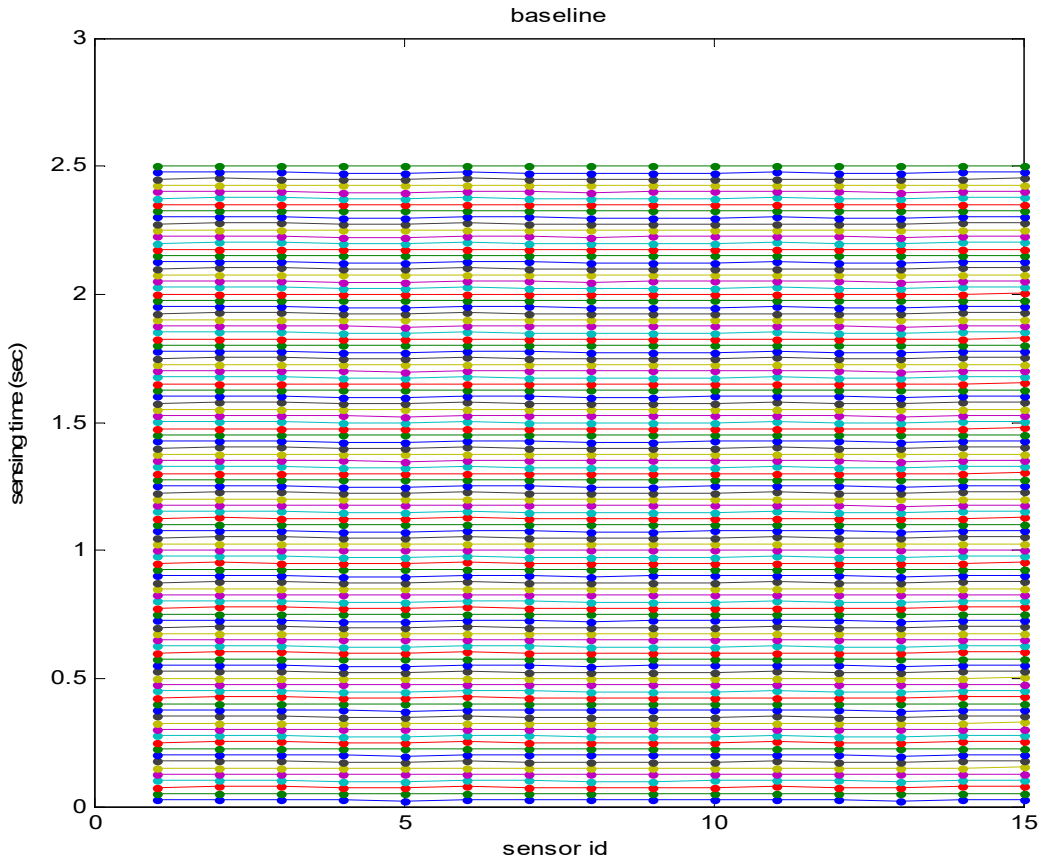


Figure 4.1: Sampling Time Instants Due To Baseline Time Shifts.

Figure 4.1 show the sampling time when baseline time shift is giving in the sampling interval for all the sensors present in cooperative communication network. In this case all the

sensors are synchronized but all of them delays equally from a fix period at each sampling instants.

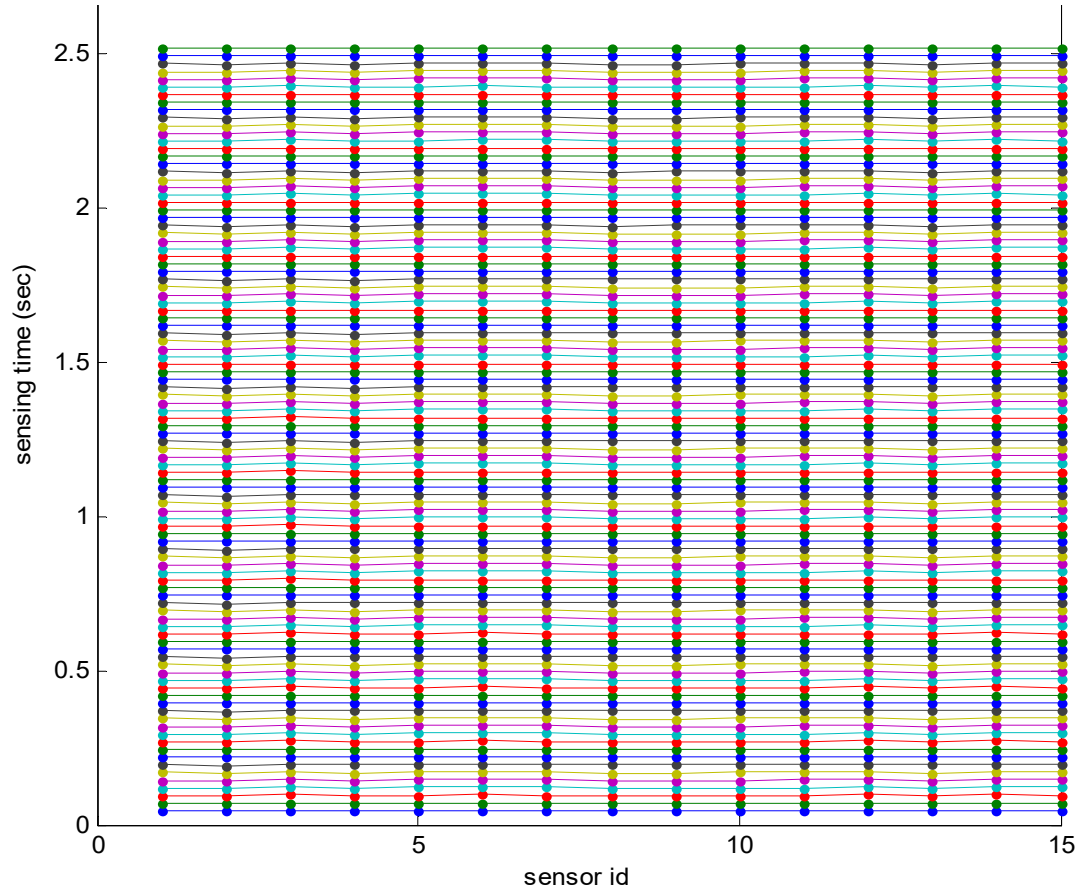


Figure 4.2: Sampling Time Instants Due To Constant Time Shifts In Cooperative Communication Network Application..

Figure 4.2 show the sampling time when constant time shift is giving in the sampling interval for all the sensors in cooperative communication network. In this case all the sensors are losing synchronism but in a constant delays or advance sensing equally from a fix period at each sampling instants on reaching at relay node.

As we can see in above figures sampling interval for each sensor is varying hence if the sensing activities are observed for long time we can find error in the sampling interval from the ideal sampling interval in cooperative communication network environment. So from the 15 sensor nodes the node having minimum error to the ideal sampling interval is considered as reference

node and after determining the mean sampling interval for each node the error in sampling instants are calculated with respect to reference node. In the case of data record for linear time shifts from table 4.2 the reference node is sensor node 8 and the average sampling interval for all nodes is given below:

$$Ts_{avg} = [0.0253, 0.0249, 0.0249, 0.0249, 0.0249, 0.0253, 0.0249, 0.0249, 0.0249, 0.0249, 0.0249, 0.0253, 0.0249, 0.0253]$$

Since the ideal sample time is 0.025sec thus we can see that there is difference in sampling time of each node.

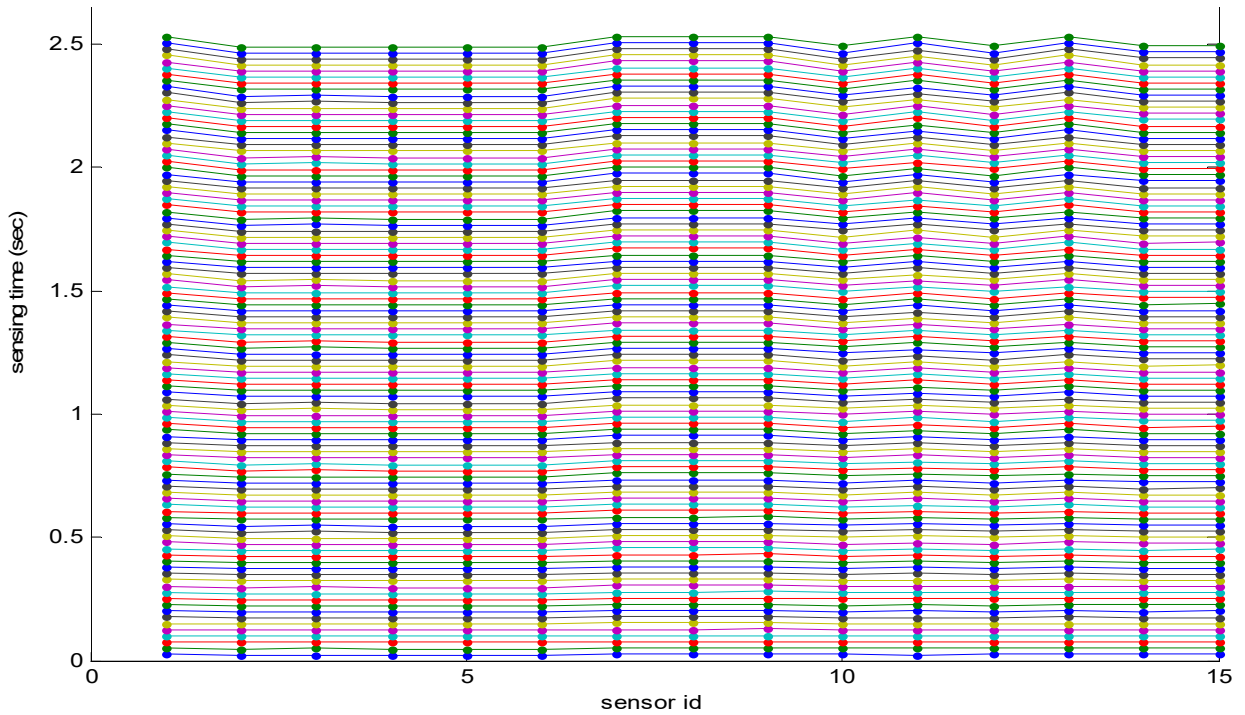


Figure 4.3: Sampling Time Instants Due To Linear Time Shifts In Cooperative Communication Network Applications.

Figure 4.3 show the sampling time when linear time shift is giving in the sampling interval for all the sensors. In this case all the sensors are losing synchronism in a high degree as sampling instants increases.

Table 4.3: Effect Of Sensing Delay In Sensor Sampling Time As Compared To Reference Node

Node id	f_{smean}	T_s mean (microsec)	%err	std dev in T_s (microsec)	Del _i (microsec)	Fractional Delay
1	39.5257	25300	1.19993	0.877668775	400.462	0.01602
2	39.5257	25300	1.19993	0.741968045	402.769	0.01611
3	40.161	24899.8	-0.40085	0.814042659	0.95087	3.80×10^{-05}
4	40.161	24899.8	-0.4008	0.782713853	1.89558	7.58×10^{-05}
5	40.161	24899.8	-0.40088	0.762717284	2.46738	9.87×10^{-05}
6	40.161	24899.8	-0.40083	0.742613617	0.41135	1.65×10^{-05}
7	39.5257	25300	1.1999	0.812101956	401.435	0.01606
8	40.161	24899.8	-0.40087	0.828429828	0	0
9	40.161	24899.8	-0.40085	0.728988204	0.95097	3.8×10^{-05}
10	40.161	24899.8	-0.40083	0.840510536	1.41536	5.66×10^{-05}
11	40.161	24899.8	-0.40084	0.840643144	0.40485	1.62×10^{-05}
12	40.161	24899.8	-0.40087	0.8509291	1.35033	5.40×10^{-05}
13	39.5257	25300	1.19988	0.727041619	400.749	0.01603
14	40.161	24899.8	-0.40082	0.6641244	2.49901	1.00×10^{-04}
15	39.5257	25300	1.19994	0.777121099	402.372	0.01609

Table 4.3 shows the %error in each sensor due to shifts in sensing intervals with respect to the reference nodes. This error is varying from -0.4 % to 1.99%. After observing the effects of delay shifts in sensor nodes we have considered two nodes sensing a time series data with a delay in their sensing instants from the ideal sampling time. The sampling time of sensor1 is $t_a = 0.025$ sec while for sensor 2, it is $t_b = 0.0247$ sec

and the linear shift delay is assumed to be $\text{del} = 0.02$ sec. The data is generated and broken into 10 segments for both sensors and shown in figure 4.4 and 4.5 in respect of different time slots. Segment 1 is from 0 to 30 sec, segment 2 is from 20 to 50 sec, segment 3 is from 45 to 75 sec and similarly other all other segments are of 30 sec but started from the points at which they have minimum error.

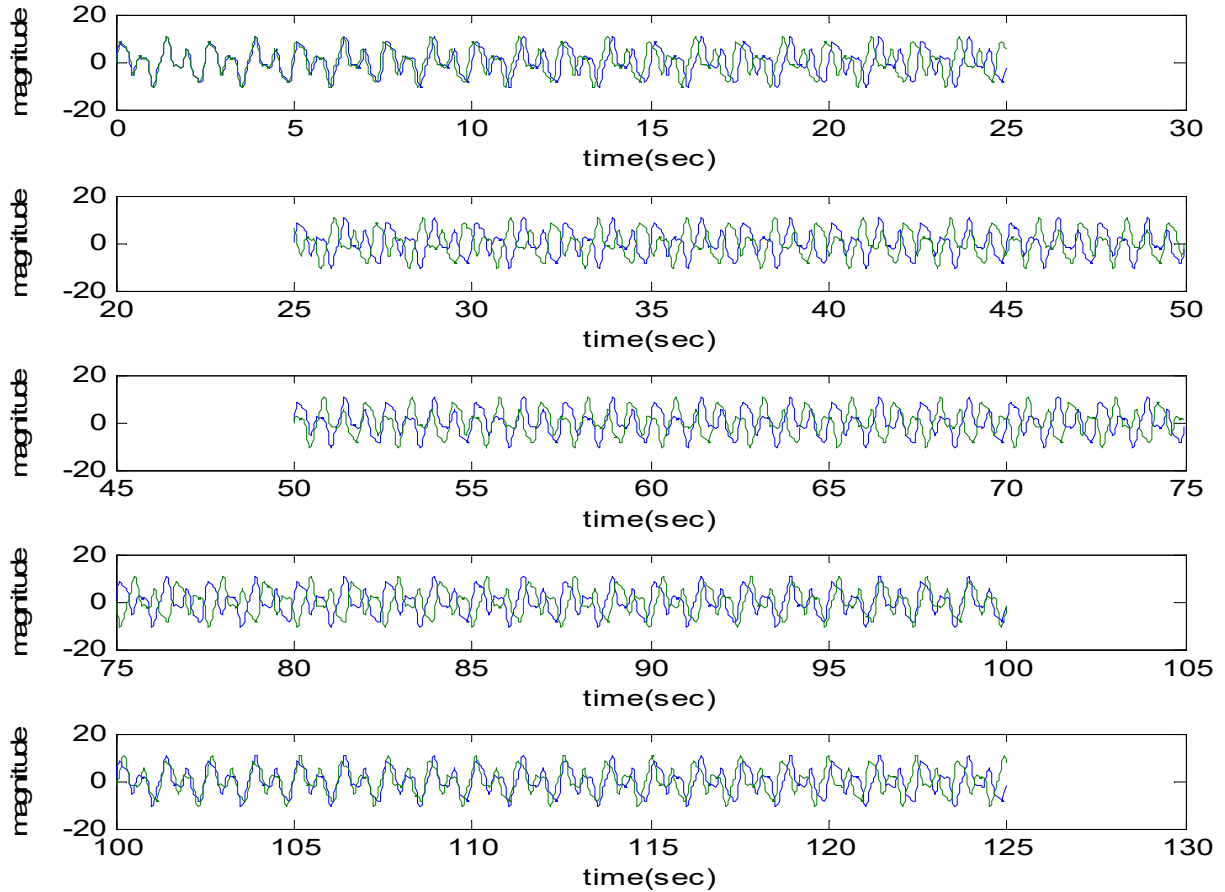


Figure 4.4: Time Series Sensor Data Segments Of Both Sensors From Segment1 To 5.

After generation of segments of sensor X1 & X2 at a given distance the data of X2 are updated by multiplication with the complex exponent delay function and CPSD determination is performed for segments of X1 & X2 without the correction and with correction in the delay.

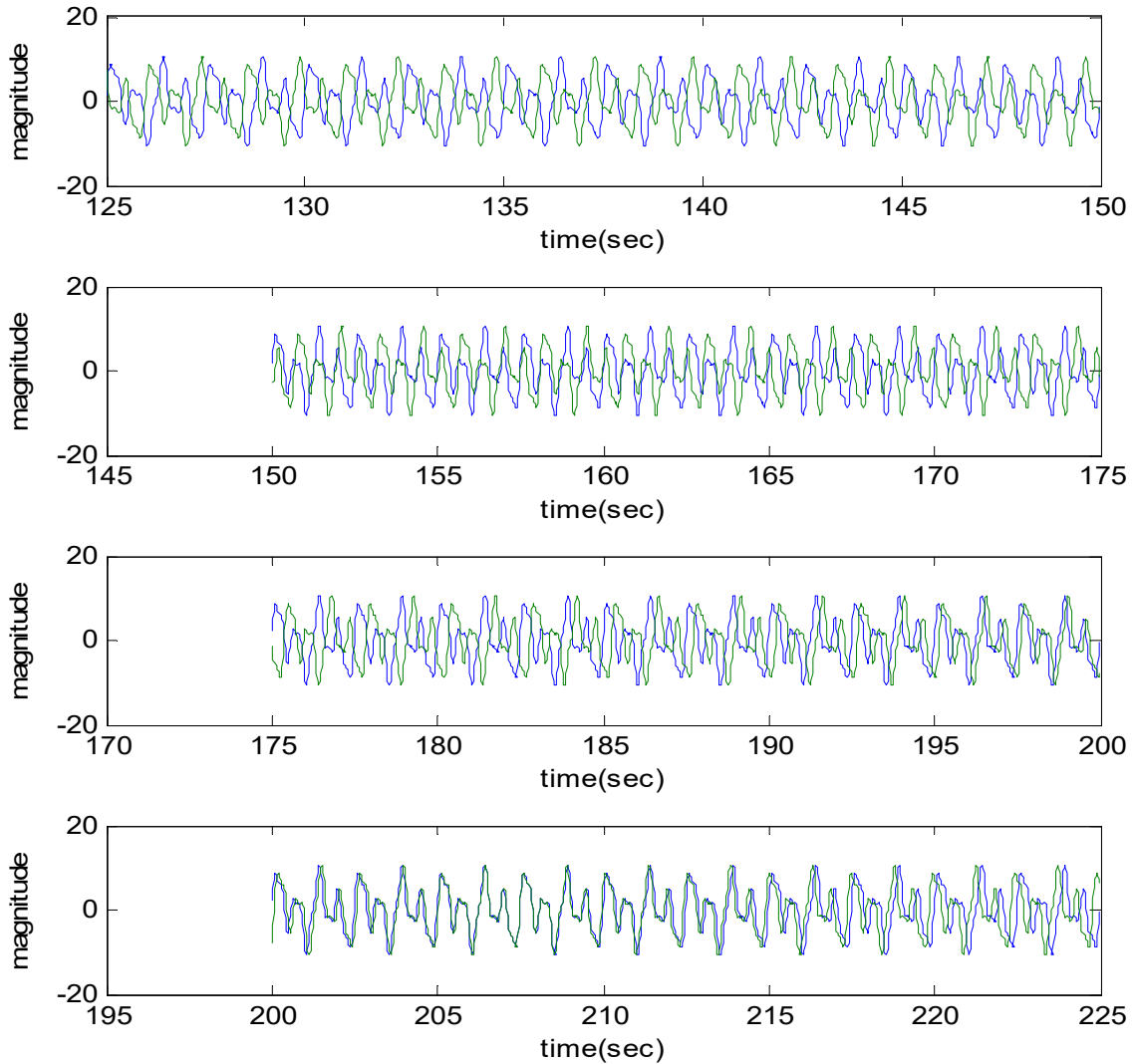


Figure 4.5: Sensed Data Time Series Segments Of Both Sensors For Segment6 To 10.

The Welch method is used to calculate the cross power spectral density estimate for all the 10 segments. Some of the CPSD spectrum plot are shown in figure 4.6. However the x axis is normalized frequency so the CPSD values are again plotted for positive frequency axis only and shown in figure 4.7.

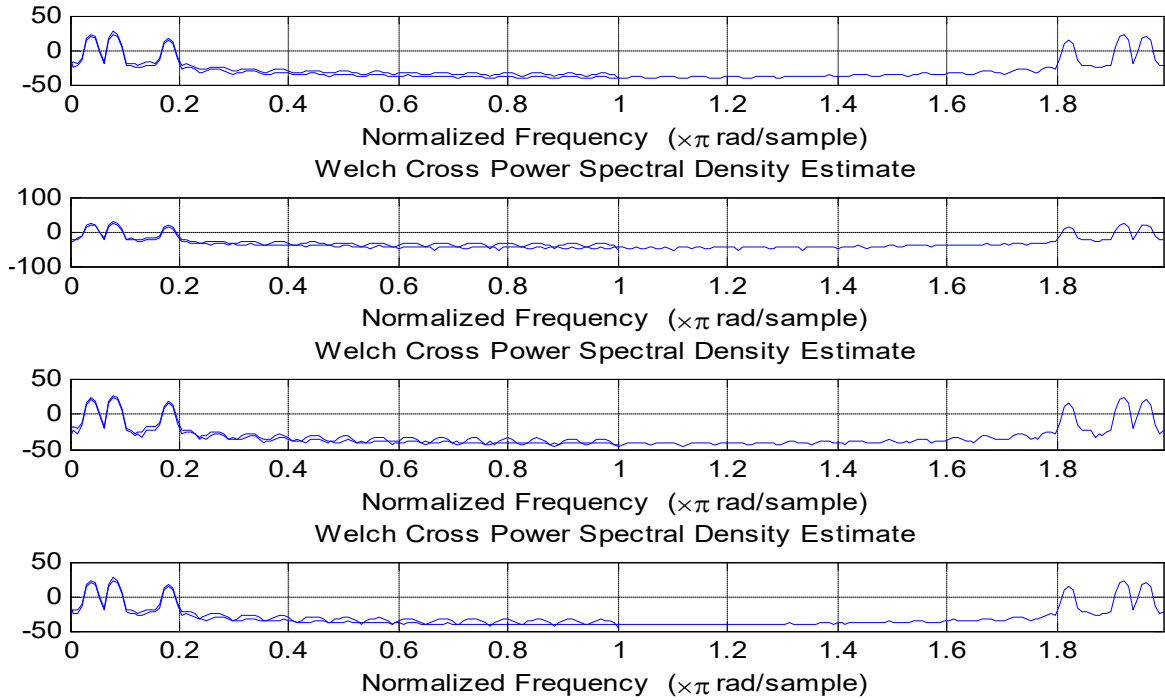


Figure 4.6: Welch Method Based Cross Power Spectral Density Estimates For Different Segments.

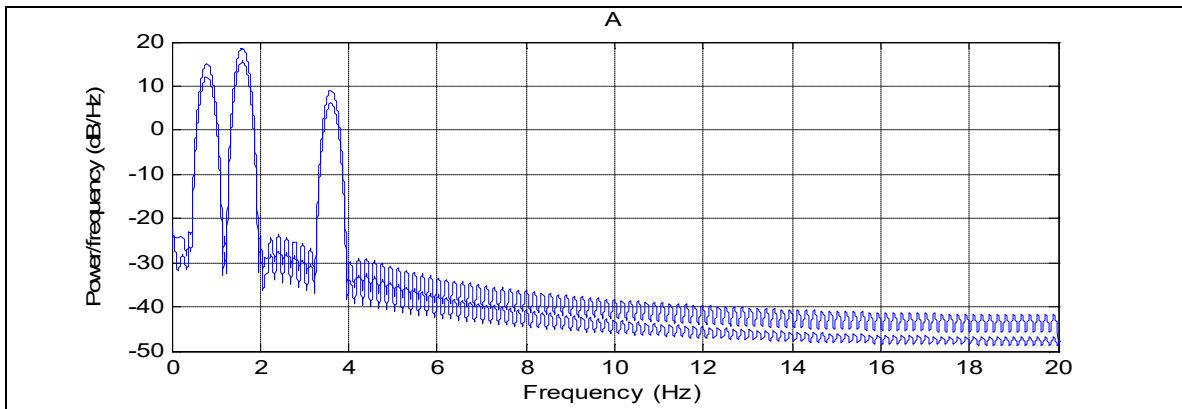


Figure 4.7 A: Cross Power Density Spectrum For Synchronized And Asynchronized Signal For Segment .

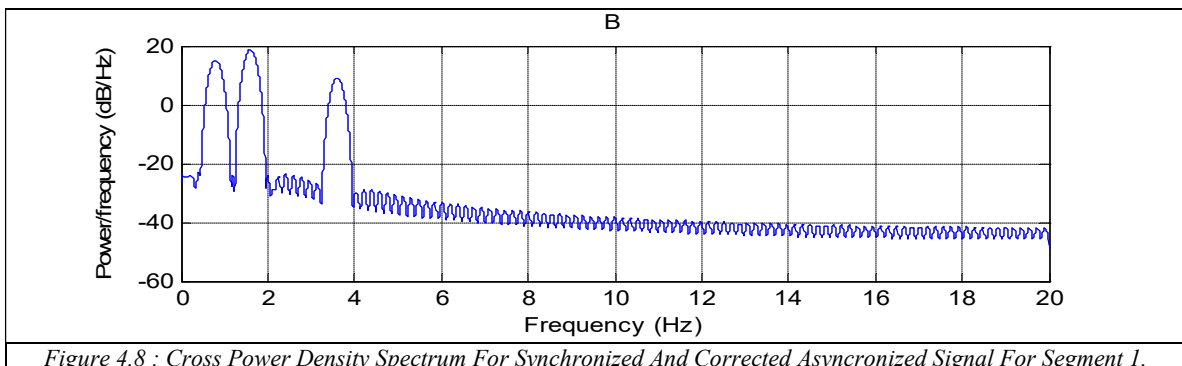


Figure 4.8 : Cross Power Density Spectrum For Synchronized And Corrected Asynchronized Signal For Segment 1.

Figure 4.7 and 4.8 shows the CPSD spectrum for delayed signals and for corrected delay signals. We can observe that in the figure 4.7 the peaks are mismatched at significant frequencies but this mismatching is eliminated in figure 4.8 for segment 1 to three. Similar observation are also found for other segments CPSD spectrums. Similarly we have applied 1-D wavelet denoising on the received signal on all the segments and then evaluated the CPSD of X1 and X2 segments to determine the peak values of spectrums and the frequency values at respective peaks. The data segments are passed

through the wavelet transforms and the wavelet decompositions produced the segment data in different components such that the signal is decomposed into several frequency component. The high frequency components are suppressed and thus the signal flickers related distortions are eliminated. Figure 5 shows the data obtained after DWT of noisy segments. These are 1 to 9 segments and each segment has 200 samples. Hence the transformed data is shown in surface plot

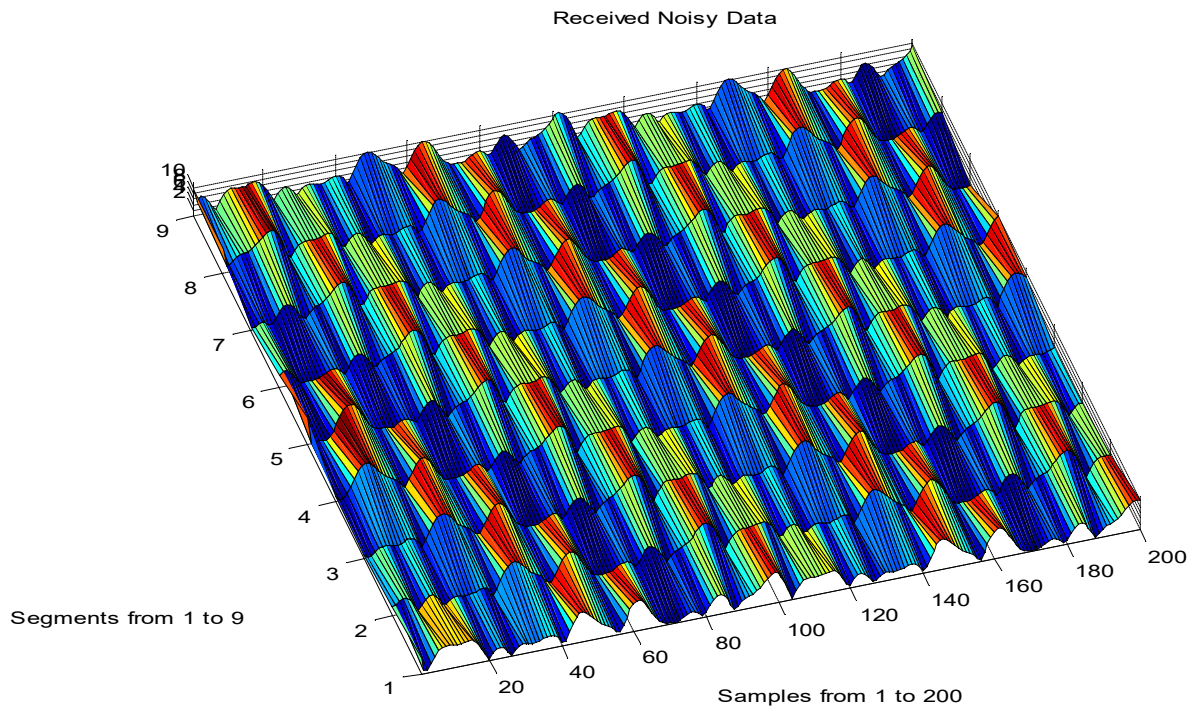


Figure 5: Segment Wise Wavelet Transform At Different Sampling Instants

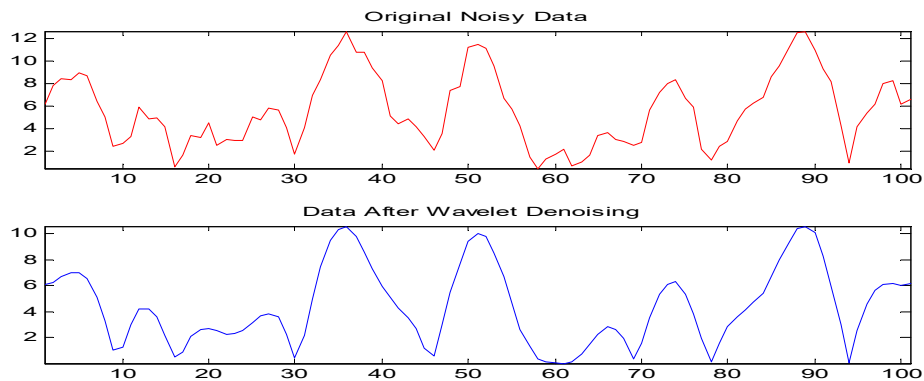


Figure 6: Data Before And After 1D DWT Denoising For Segment 1.

After applying the wavelet denoising the CPSD in between segments of X1 and X2 received signal is evaluated by Welch method. The peak finding command is used for determining the cross power spectrum magnitude and the respective frequency index and the frequencies are determined for both data i.e peak finding data of signal; without applying 1-D DWT denoising and with applying denoising. The results are tabulated below for each segments:

Table 4.4 (a) Measurements of modal shape of Segments in terms of peaks:

Actual Peak	Observed Peak a	Peak a error	Observed Peak b	Peak b error
0.02	0.02	0.00	0.01	0.01
0.02	0.03	-0.01	0.01	0.01
51.75	0.10	51.64	51.55	0.20
202.75	201.87	0.89	202.79	-0.03
433.75	430.08	3.59	433.88	-0.21

Table 4.4 (b) Measurements of modal shape of Segments in terms of frequency:

Actual Frequency	Observed Frequency a	Frequency a error	Observed Frequency b	Frequency b error
0	0	0	0	0
0.16	0.16	0	0.16	0
0.31	0.31	0	0.31	0
0.47	0.47	0	0.47	0
0.63	0.63	0	0.63	0

5. IMPORTANCE AND NOVELTY:

Prior works generally focused on simple wireless networks without the heterogeneity introduced due to relay nodes. The previous works only corrected the time shift but no focus is paid in denoising prior to delay correction [24-27]. The resource of synchronization error in data information are generally semiconductor junction delay in switching moments and in real time these time shifts have different behaviour as compared to simulated resources of random errors in this paper. Hence the performance results may have limited amount of a reliability and the foolproof solution may only be justified on running at real time behaviour. The Internet of Things has attracted a lot of attention in the

modern period due to its numerous and promising applications in several fields. Cooperative communication serve as the core communication backbone for omnipresent settings in the future. The purpose of this work's literature survey is to conduct a feasibility analysis of the Internet of Things, and it is found that cooperative communication will continue to evolve along with high-level technological advancements in wireless communications, digital circuit design, and micro-electromechanical systems. We have noticed that the in cooperative communication time synchronization is a crucial issue for preserving data coordination, consistency, and performance quality of other essential operations responses, such as power management, security, and data fusion and scheduling in IoT applications.

6. CONCLUSION AND FUTURE WORK

The goal of this study is to provide a method for assessing and reducing non-synchronous sensing defects in sensor nodes utilising modal identification techniques using the MATLAB platform in cooperative communication applications. It is observed that while using the DWT denoising prior to spectral characteristics based correction the frequency error are reduced or almost converged to zero. It has give high accuracy by nullifying the synchronization mismatch. The reasons of baseline, constant shift, and linear shift non-synchronous sensing are first addressed, followed by simulations for a group of sensors with sampling time delays. On the basis of data gathered by the sensors, the consequences of this delay are first detected, and then their effects on frequency and peak spectrum are estimated. The two errors most noticeable for causing non-synchronous behaviour are non-simultaneous sensing activity at startup and variations in sampling frequency over the whole sensor. The algorithm's simulation results led researchers to the conclusion that these flaws could distort the results and lead to inaccurate estimations of frequency and spectrum modal shape. The algorithm suggests a new approach for removing errors caused by sensor synchronization loss at sampling time, combining 1D wavelet denoising and Welch power estimation. The signal segments are chosen using this process at the closest sampling time inaccuracy. Then, using non-synchronous samples, it estimates the cross power spectral density (PSD) of segments produced by a pair of sensors' output responses

and uses the Welch technique of spectrum estimation based on an FFT to the received segments after applying 1D dwt denoising. This approach produces the corrected cross spectral density, which is used in the IFFT formulation to express the correlation functions. As a result, the corrected CPSDs are frequency domain representational of correlation functions and can be used in a variety of ways in subsequent work as a rectified output for modal identification, frequency estimation, and pattern recognition algorithms. The current raw synchronous time history estimate procedure is straightforward, more accurate, and computationally economical when compared to conventional methods of peak discovery just employing CPSD without denoising. Simulations of validated programming make up the suggested methodology. Based on synchronous data, the simulation findings match the frequency and important peak-like properties. The cooperative communication system based simulation demonstrated the presence of error in spectral estimates due to mismatch in sampling time of sensor nodes. This paper demonstrated an approach that efficiently minimizes the mismatch in sampling delay to mitigate their impact on synchronization error of the cooperative communication network; ii) spectral characteristics application in sampled sequences delay correction provided high accuracy in estimate of sample time mismatch iii) evaluate of DWT based denoising prior to correction of time delay shift give better results.

The application of this work focused on a special case of vibration measurements using sensor nodes under cooperative environment. This research requires accurate reading of frequency of vibration and the magnitude of specific frequency that may seriously damage a civil structure. This kind of application is untouched and critical analysis are highly important to defend the serious accidents due to collapse of buildings ,bridges etc because of aging, overloading or natural disasters.

REFERENCES:

- [1] A. Nayak and I. Stojmenovic, "Wireless Sensor and Ac- tuator Networks: Algorithms and Protocols for Scalable Coordination and Data Communication," Wiley, 2010.
- [2] W. Heinzelman, A. Chandrakasan and H. Balakrishnan, "An Application-Specific Protocol Architecture for Wire- less Microsensor Networks," IEEE Transactions on Wire- less Communications, October 2002, pp. 660-670.
- [3] Anne-Claire Boury-Brisset, "Ontology-based Approach for Information Fusion".
- [4] M. Beldjehem, "On Conception and Validation of Hybrid Relational Min-Max Learners," International Journal of Hybrid Information Technology, Vol. 4, No. 3, 2011, pp. 1-21.
- [5] S. I. Matta and A. Bestavros, "SEP: A Stable Election Protocol for Clustered Heterogeneous Wireless Sensor Networks," Technical Report BUCS-TR-2004-022G.
- [6] W. Heinzelman, A. Chandrakasan and H. Balakrishnan, "Energy-Efficient Communication Protocol for Wireless Microsensor Networks," Proceedings of the 33rd Hawaii International Conference on System Sciences, 4-7 January 2000.
- [7] S. Hussain and A. W. Matin, "Energy Efficient Hierar- chical Cluster-Based Routing for Wireless Sensor Net- works," Jodrey School of Computer Science Acadia Uni- versity Wolfville, Nova Scotia, 2005, pp. 1-33.
- [8] K. Ghosh, P. P. Bhattacharya and P. Das, "Effect of Mul- tipath Fading and Propagation Environment on Perform- ance of a Fermat Point Based Energy Efficient Geocast Routing Protocol," International Journal of Wireless & Mobile Networks, Vol. 4, No. 1, 2012, pp. 215-224.
- [9] H. Shpungin, "Feasible Capacity of Distributed Beam- forming in Multi-Hop Wireless Sensor Networks," Mo- bile Adhoc and Sensor Systems (MASS), IEEE 8th Inter- national Conference, Valencia, 17-22 October 2011, pp. 19-24.
- [10] G. Chen, C. Li, M. Ye and J. Wu, "An Unequal Cluster- Based Routing Protocol in Wireless Sensor Networks," Wireless Networks, Vol. 15, No. 2, 2009, pp. 193-207.
- [11] H. Chen and S. Megerian, "Cluster Sizing and Head Se- lection for Efficient Data Aggregation and Routing in Sensor Networks," IEEE Wireless Communications and Networking

- Conference, Las Vegas, 3-6 April 2006, pp. 2318-2323.
- [12] S. Soro and W. B. Heinzelman, "Cluster Head Election Techniques for Coverage Preservation in Wireless Sensor Networks," *Ad Hoc Networks*, Vol. 7, No. 5, 2009, pp. 955-972
- [13] K. Ghosh, S. Roy and P. K. Das and I. Min, "An Intelligent Fermat Point Based efficient Geographic Packet Forwarding Technique for Wireless Sensor and Ad Hoc Networks," *International Journal on Applications of Graph Theory in Wireless Adhoc Networks and Sensor Networks (GRAPH-HOC)*, Vol. 2, No. 2, 2010, pp. 34-44.
- [14] Dilip Kumar et. al., "A Novel Multihop Energy Efficient Heterogeneous Clustered Scheme for Wireless Sensor Networks" *Tamkang Journal of Science and Engineering*, Vol. 14, No. 4, pp. 359368 (2011).
- [15] O. Younis and S. Fahmy, "HEED: A Hybrid, Energy-Efficient, Distributed Clustering Approach for Ad-hoc Sensor Networks," *IEEE Transaction on Mobile Computing*, Vol. 3, No. 4, 2004, pp. 366-379.
- [16] W. Heinzelman, A. Chandrakasan and H. Balakrishnan, "An application-specific protocol architecture for wireless microsensor networks," *IEEE Transactions on Wireless Communications* 1(4) (2005) 660-670.
- [17] W. Heinzelman, A. Chandrakasan, and H. Balakrishnan, "Energy-efficient routing protocols for wireless microsensor networks," in *Proc. 33rd Hawaii Int. Conf. System Sciences (HICSS)*, Maui, HI, Jan. 2000.
- [18] Katayoun Sohrabi, et. al., "Protocols for Self-Organization of a Wireless Sensor Network", the 37th Allerton Conference on Communication, Computing and Control, September 1999.
- [19] Shalli Rani et. al. "EEICCP—Energy Efficient Protocol for Wireless Sensor Networks", *Wireless Sensor Network*, 2013, 5, 127-136
- [20] Dilip Kumar et. al., "A Novel Multihop Energy Efficient Heterogeneous Clustered Scheme for Wireless Sensor Networks" *Tamkang Journal of Science and Engineering*, Vol. 14, No. 4, pp. 359368 (2011)
- [21] D. Hall, *Mathematical Techniques in Multisensor Data Fusion*. Boston, MA: Artech House, 1992.
- [22] W. Heinzelman, "Application-specific protocol architectures for wireless networks," Ph.D. dissertation, Mass. Inst. Technol., Cambridge, 2000.
- [23] L. Hu, "Distributed code assignments for CDMA packet radio networks," *IEEE/ACM Trans. Networking*, vol. 1, pp. 668-677, Dec. 1993.
- [24] Anand Ranjan, O.P. Singh, G. R. Mishra, H. Katiyar, "Optimal Relay Node Selection Using Multi-objective based Lion Optimization Algorithm for Multiuser Cooperative Communication Network," *International Journal of Advanced Science and Technology*, Vol 29, No. 5, 2020 pp. 11867-11884.
- [25] Anand Ranjan, O. P. Singh, G. R. Mishra, H. Katiyar, "Multi-objective optimization for performance analysis of Cooperative Wireless Communication Multi-objective optimization for performance analysis of Cooperative Wireless Communication," *International Journal of Advanced Trends in Computer Science and Engineering*, Vol 9, Number-5, 2020, pp. 7636-7644, DOI: 10.30534/ijatcse/2020/103952020.
- [26] Anand Ranjan, O. P. Singh, H. Katiyar, "Broadband Spectrum Channels Sensing For Co-operative Network Using Sub Sampling Subspace Estimation Approach," *Journal of Theoretical and Applied Information Technology*, Volume 100, pp. 1558-1570.
- [27] A. Ranjan, O.P. Singh, H. Katiyar, "Improved Security Mechanism For Spectrum Handoff In Cooperative Wireless Networks," *Journal Of Theoretical and Applied Information Technology*, Vol. 100, pp. 5107-5118